

RESEARCH

Open Access



# Butyrate induces higher host transcriptional changes to inhibit porcine epidemic diarrhea virus strain CV777 infection in porcine intestine epithelial cells

Zhen Zhong<sup>1</sup>, Yaqin Zhang<sup>1</sup>, Xuting Zhao<sup>1</sup>, Chunbao Zhou<sup>1</sup>, Shubin Zhu<sup>1</sup> and Jiayun Wu<sup>1\*</sup>

## Abstract

Newborn piglets' health is seriously threatened by the porcine epidemic diarrhea virus (PEDV), which also has a significant effect on the pig industry. The gut microbiota produces butyrate, an abundant metabolite that modulates intestinal function through many methods to improve immunological and intestinal barrier function. The objective of this investigation was to ascertain how elevated butyrate concentrations impacted the host transcriptional profile of PEDV CV777 strain infection. Our findings showed that higher concentrations of butyrate have a stronger inhibitory effect on PEDV CV777 strain infection. According to RNA-seq data, higher concentrations of butyrate induced more significant transcriptional changes in IPEC-J2 cells, and signaling pathways such as PI3K-AKT may play a role in the inhibition of PEDV CV777 strain by high concentrations of butyrate. Ultimately, we offer a theoretical and experimental framework for future research and development of novel approaches to harness butyrate's antiviral infection properties.

**Keywords** Pigs, Porcine epidemic diarrhea virus, Butyrate, RNA-seq

## Introduction

Porcine epidemic diarrhea (PED) is an acute, highly contagious and contact intestinal disease caused by porcine epidemic diarrhea virus (PEDV) that affects pigs of all ages and is mainly characterized by vomiting, watery diarrhea and dehydration in infected pigs. Piglets are highly morbidly and fatally affected by PEDV infection, which primarily affects small intestine epithelial cells in vivo. Most of the infected piglets die within 7 days after birth, and the mortality rate of young piglets was as high as 80% [1]. Since 2010 and 2013, PED outbreaks in East

Asia and North America have rekindled interest in the 1978-discovered swine coronaviruses [2]. PEDV belongs to the genus *Alphacoronavirus* of the Coronavirus family, which is approximately 28 kb in length (excluding the poly A-tail) that encodes four structural proteins and nonstructural proteins [3]. One of the main methods to prevent PEDV infection in pigs since the PED outbreak has been vaccination. However, since 2010, the emergence of highly mutated PEDV strains has seriously hampered the effectiveness of vaccination, and the use of vaccines has not been able to lower the incidence and lethality of PEDV in piglets [4]. The search for new anti-PEDV strategies is now crucial to the pig industry's continued growth.

Numerous studies and clinical observations have demonstrated the importance of the gut microbiota in the

\*Correspondence:

Jiayun Wu

wujayun@jsahvc.edu.cn

<sup>1</sup>Jiangsu Agri-Animal Husbandry Vocational College, Taizhou 22530, China



© The Author(s) 2024. **Open Access** This article is licensed under a Creative Commons Attribution 4.0 International License, which permits use, sharing, adaptation, distribution and reproduction in any medium or format, as long as you give appropriate credit to the original author(s) and the source, provide a link to the Creative Commons licence, and indicate if changes were made. The images or other third party material in this article are included in the article's Creative Commons licence, unless indicated otherwise in a credit line to the material. If material is not included in the article's Creative Commons licence and your intended use is not permitted by statutory regulation or exceeds the permitted use, you will need to obtain permission directly from the copyright holder. To view a copy of this licence, visit <http://creativecommons.org/licenses/by/4.0/>. The Creative Commons Public Domain Dedication waiver (<http://creativecommons.org/publicdomain/zero/1.0/>) applies to the data made available in this article, unless otherwise stated in a credit line to the data.

pathophysiology of acute respiratory distress syndrome and sepsis, and the development of numerous diseases is linked to the decrease of gut bacterial diversity that results in ecological dysregulation [5, 6]. Functionally, these alterations in the microbiota's makeup have been linked to a reduction in the synthesis of short-chain fatty acids (SCFAs). It has been shown that the number of microorganisms involved in SCFAs production, including *E. faecalis*, *Clostridium perfringens* and *Fusobacterium cholerae*, is reduced in fecal samples from COVID-19 patients compared to healthy controls. Therefore, there is proof that alterations in the microbiota, such as a decrease in SCFA-producing bacteria, are linked to the existence and/or infection of SARS-CoV-2 in the gut [7]. Studies have not been conducted to determine whether these modifications' impact on SCFAs is connected to infection.

The gut microbiota constitutes the assemblage of microorganisms residing in the gastrointestinal tract of animals, and it plays a crucial role in maintaining the overall well-being of the host organism. SCFAs are produced through the process of fermenting dietary fiber. They are saturated fatty acids that have a carbon chain length ranging from one to six atoms [8]. SCFAs play a crucial role in facilitating the interaction between the host and the microbiota. Previous research has documented the capacity of these molecules to modulate the synthesis of antimicrobial peptides and mucus, as well as influence intestinal permeability and activate the mucosal immune system [9]. Furthermore, it is important to note that SCFAs have a positive impact on gastrointestinal health. Additionally, SCFAs that are produced in the intestine are easily absorbed into the bloodstream and play a crucial role in regulating various organ functions. These functions include energy utilization and metabolism, inflammation, as well as the regulation of the gut-brain axis [10, 11].

A previous study has demonstrated that low concentrations of SCFAs ranging from 10  $\mu$ M to 1 mM can effectively inhibit the replication of PEDV [12]. However, this study did not investigate the functional mechanism of high concentrations of SCFAs, and the roles and mechanisms of high-concentration SCFAs in porcine coronaviruses, particularly in PEDV, remain unclear. Therefore, the present study aimed to examine the impact of various high concentrations of SCFAs on the replication of PEDV. Specifically, the study focused on investigating the effects of elevated levels of butyrate on the transcriptional regulation of porcine small intestinal epithelial (IPEC-J2) cells during PEDV infection. Furthermore, we have placed significant emphasis on the emerging role of gut-derived metabolites in the infection process of PEDV, with the aim of providing valuable recommendations for future breeding efforts focused on disease resistance.

## Materials and methods

### Cell lines, virus, and plasmids

IPEC-J2 cells were generously provided by Prof. Wenbin Bao from Yangzhou University. IPEC-J2 cells were grown in DMEM (Thermo Fisher Scientific, Waltham, MA) supplemented with 10% FBS (GIBCO) and 1% penicillin/streptomycin (Invitrogen, Waltham, MA) at 37 °C with 5% CO<sub>2</sub>. IPEC-J2 cells underwent pretreatment with SCFAs, specifically 10 mM acetate, 10 mM propionate, and 5 mM butyrate, for a duration of 24 h before being infected with the virus. The PEDV CV777 strain was maintained by our laboratory and cultured in Vero cells following the previously described protocol [13]. Briefly, when Vero cells were cultured to a density of about 90%, PEDV was added and incubated for 2 h, the virus supernatant was then removed, and the culture medium was replenished. After 72 h, the virus solution was frozen and thawed three times, centrifuged, and filtered with a 0.45  $\mu$ m filter. Regarding the PEDV infection in IPEC-J2 cells, the cells were subjected to PEDV infection at a multiplicity of infection (MOI) of 0.1. The PEDV inoculum was removed at 2 h post-infection (hpi), and the cells were subsequently collected at 24 hpi for further experimentation.

### Cell viability assay

IPEC-J2 cells were seeded into 96-well plates at a density of  $3 \times 10^3$  cells/well. They were treated with SCFAs at concentrations of 0, 0.5, 1, 2, 5, 10, and 20 mM. The cells were then analyzed using a Cell Counting Kit-8 (Beyond Biotechnology) 24 h after inoculation. To each well, 10  $\mu$ L of CCK-8 solution was added and incubated in an incubator for 2 h. Absorption was detected at 450 nm using a microplate reader.

### Real time-quantitative PCR

The extraction of total RNA of IPEC-J2 cells was conducted using the Trizol method. Complementary DNA (cDNA) synthesis was performed using the PrimeScript RT reagent kit (TaKaRa). Real-time quantitative PCR (RT-qPCR) was performed using the qPCR SYBR Green Master Mix (Vazyme). The PEDV *M* gene primer was designed using the Primer Premier 5.0 software (Premier Biosoft, Palo Alto, CA, USA). The forward primer sequence is 5'-TCCCGTTGATGAGGTGAT-3', and the reverse primer sequence is 5'-AAGCATTGACTGAAC GACC-3'. GAPDH was employed as the reference gene for RT-qPCR. The forward primer sequence used was 5'-ACATCATCCCTGCTTCTACTGG-3', and the reverse primer sequence employed was 5'-CTCGGACGCCTGCTTAC-3'. The relative quantification results were determined utilizing the comparative Ct (2<sup>- $\Delta\Delta$ Ct</sup>) method.

### Western blot assay

IPEC-J2 cell proteins were extracted and quantified using the BCA protein assay kit (Beyotime Biotechnology). A total of 20 µg of protein was separated on 10% SDS-PAGE gels and subsequently transferred to 0.22 µm PVDF membranes (Millipore). The membranes were blocked with 5% skim milk powder and subsequently incubated with PEDV N antibodies (Medgene Labs) and GAPDH antibodies (Proteintech) at a temperature of 4 °C overnight. The membranes were subsequently incubated with the appropriate secondary antibodies, and an enhanced chemiluminescence (ECL) detection system from Bio-Rad was employed to visualize the protein bands.

### TCID<sub>50</sub> assay to detect titration of PEDV

The culture supernatants of the PEDV-infected cells under different SCFAs treatments were collected after 24 h of infection and serially diluted at a 10-fold ( $10^0$ – $10^{-7}$ ) dilution. Vero cells were seeded into 96-well plates and added with 100 µL of serial dilutions of PEDV. PEDV-infected cells were cultured for 6 days, and the cytopathic effect was observed daily. Viral titers were quantified using the Reed–Muench method, which measures the 50% tissue culture infectious dose (TCID<sub>50</sub>).

### Data analysis of RNA-seq

IPEC-J2 cells were seeded in 6-well plates, after reaching 90–100% confluence, 5 mM butyrate was pretreated for 24 h. The control group was left untreated. Subsequently, the cells were infected with PEDV using a MOI of 0.1 for 24 h. The cells were then collected and divided into 4 groups: butyrate treatment+PEDV infection, butyrate treatment only, PEDV infection only, and negative control (NC), with 3 replicates in each group. RNA isolation of IPEC-J2 cells was performed followed by the Trizol method. Duplicate samples were obtained and utilized to construct the library using the NEBNext® ultra™ RNA library prep kit for Illumina® (NEB). The AMPure XP system (Beckman Coulter) was employed for the purification of fragments with a length ranging from 250 to 300 bp. The PCR process was subsequently conducted. The Agilent Bioanalyzer 2100 system (Agilent Technologies), was employed for the purification of the PCR products. RNA-seq analysis was conducted using an Illumina HiSeq platform following established protocols. The threshold for statistical significance was set as a *P*-adjust value < 0.05.

### Enrichment analysis

Data normalization was carried out by LOWESS fitting on an M versus A plot [14]. KEGG analysis was performed to explore the pathways enriched with differentially expressed genes (DEGs). The DEGs were analyzed using the Kyoto Encyclopedia of Genes and Genomes

(KEGG) database to identify all the pathway terms involved. The significance level of each pathway term was calculated using the Fisher test, and pathway terms with a *P*-adjust value < 0.05 were considered statistically significant.

### Statistical analysis

Data were analyzed by SPSS software for statistical analysis. A two-sided Student's *t*-test was used to analyze the differences between the two groups, and standard analysis of variance (ANOVA) was used for more than three groups. In all analyses, \**P* < 0.05; \*\**P* < 0.01; \*\*\**P* < 0.001 for the comparison of the indicated treatments.

## Results and analysis

### SCFAs promote PEDV CV777 strain replication in IPEC-J2 cells

Previous research has demonstrated that low levels of SCFAs can effectively hinder the infection of PEDV in IPEC-J2 cells. However, the impact of high concentrations of SCFAs on PEDV infection has not been explored yet. Therefore, this study aimed to further investigate the impact of elevated levels of SCFAs on PEDV CV777 strain infection. We initially investigated the impact of SCFAs on IPEC-J2 cell activity. The CCK-8 assay revealed that acetic acid did not inhibit IPEC-J2 cell activity at 20 mM, while propionic acid significantly inhibited IPEC-J2 activity at 20 mM (*P* < 0.05). Moreover, butyric acid exhibited a significant inhibitory effect on IPEC-J2 cells even at 10 mM (*P* < 0.01) (Fig. 1A). Therefore, 10 mM acetate, 10 mM propionate, and 5 mM butyrate were selected for pretreating IPEC-J2 cells for 24 h before infection with PEDV at MOI of 0.1 in this study. The findings indicated that elevated levels of SCFAs significantly inhibited the expression of the PEDV *M* gene (*P* < 0.05) (Fig. 1B). Additionally, the western blot analysis demonstrated a notable inhibition in the expression of the PEDV N protein (Fig. 1C). The TCID<sub>50</sub> results indicated that all three SCFAs significantly reduced the viral titer of PEDV (*P* < 0.001). Light microscopic observations showed that the lesions were most prominent in IPEC-J2 cells that were not treated with SCFAs. Among the SCFAs examined, it was found that butyrate exhibited the most pronounced impact.

### Butyrate affects the transcription of IPEC-J2 cells more than PEDV CV777 strain infection

In this study, a follow-up investigation was conducted to examine the mechanism through which butyrate influences PEDV infection. RNA-seq was employed to analyze the transcriptional alterations in IPEC-J2 cells following PEDV infection after pre-treatment with butyrate. The PCA results demonstrated a clear distinction among the individual treatment groups (Fig. 2A). Additionally, the

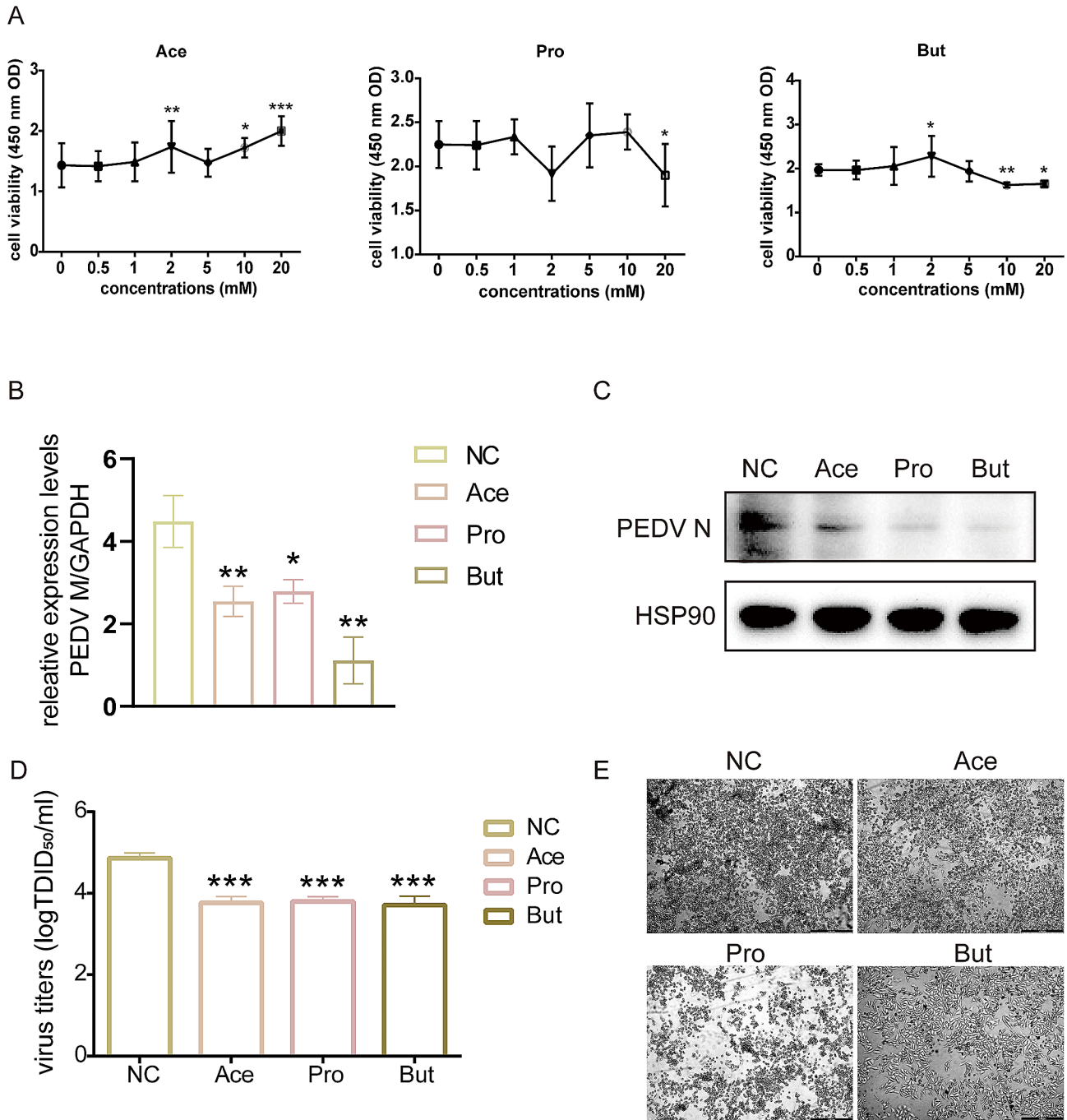


**Fig. 1** Illustrates the promotion of PEDV replication in IPEC-J2 cells by SCFAs. **(A)** Effect of SCFAs on IPEC-J2 cell viability detected by CCK-8 assay,  $n=6$ . **(B)** The impact of various SCFAs on the expression of the PEDV *M* Gene. **(C)** The impact of various SCFAs on PEDV N protein expression. **(D)** TCID<sub>50</sub> assay was used to determine PEDV virus titers among SCFAs treatments and negative control groups. Viral titers were quantified by a TCID<sub>50</sub> using the Reed–Muench method. **(E)** IPEC-J2 cell lesion diagram. Light microscopy was used to observe lesions in SCFAs-pretreated and PEDV-only infected IPEC-J2 cells 24 h after PEDV infection. The rounded, crumpled cells are the diseased cells. Experiments for B-C were first performed by pre-treating IPEC-J2 cells with 10 mM acetate, 10 mM propionate, and 5 mM butyrate for 24 h followed by 24 h of PEDV infection. NC: negative control, Ace: Acetate, Pro: Propionate, But: Butyrate. \* $P < 0.01$ ; \*\*\* $P < 0.001$

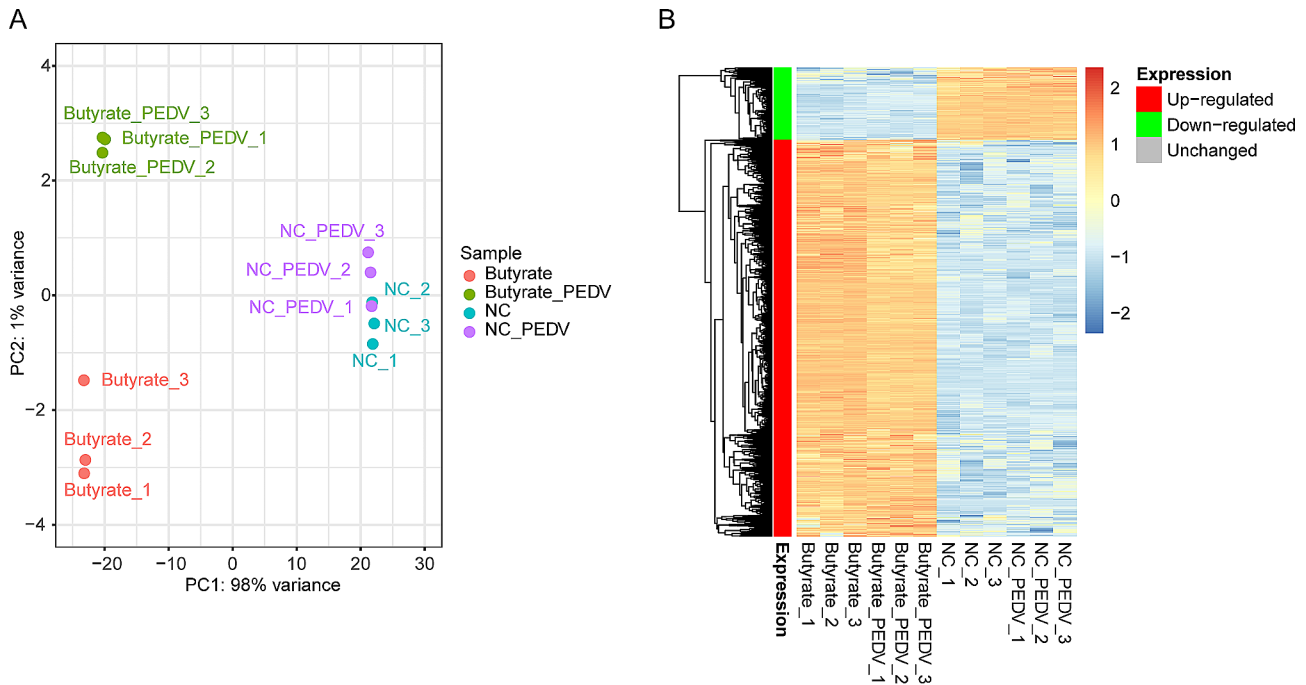


**Fig. 2** Overall transcriptional alterations in IPEC-J2 cells induced by the administration of butyrate during the process of PEDV infection. **(A)** PCA analysis of all RNA-seq samples. **(B)** Heatmap of gene expression across various groups. For RNA sequencing, IPEC-J2 cells were pretreated by 5 mM butyrate for 24 h, the control group was left untreated. Subsequently, the cells were infected with PEDV using a MOI of 0.1 for 24 h. The cells were then collected and divided into 4 groups: butyrate treatment + PEDV infection, butyrate treatment only, PEDV infection only, and negative control (NC), with 3 replicates in each group

heatmap analysis revealed a notable up-regulation tendency in most of the genes following butyrate treatment, while the impact of PEDV on the host genes was comparatively less pronounced than that of butyrate treatment (Fig. 2B).

**Gene transcription alterations in IPEC-J2 cells after PEDV CV777 strain infection**

The DEGs between the PEDV-infected group and the control group were analyzed. A threshold of *P*-adjust value < 0.05 was set, and it was found that a total of 270 up-regulated DEGs and 120 down-regulated DEGs were detected after PEDV infection (Fig. 3A). Cluster analysis revealed distinct expression patterns of the expression of these DEGs in the butyrate-treated group (Fig. 3B). Subsequent enrichment analysis of these DEGs demonstrated that the up-regulated DEGs were primarily enriched in signaling pathways such as PI3K-AKT and Rap signaling pathways (Fig. 3C). Conversely, the down-regulated DEGs were predominantly enriched in signaling pathways related to protein processing in the endoplasmic reticulum and prion disease (Fig. 3D).

**The impact of butyrate treatment on gene transcription in IPEC-J2 cells**

We conducted a further analysis of the DEGs between the group treated with butyrate and the control group. Given

that butyrate treatment induced a broader spectrum of transcriptional alterations in host genes, we adjusted the threshold to *P*-adjust value < 0.05,  $|\log_2\text{fold change}| > 2$ . Consequently, we identified a total of 1,643 DEGs were up-regulated following butyrate treatment, while 278 DEGs were down-regulated (Fig. 4A). Cluster analysis revealed that these DEGs were primarily influenced by the administration of butyrate (Fig. 4B). Subsequent enrichment analysis of these DEGs demonstrated that the up-regulated DEGs were predominantly enriched in signaling pathways related to neuroactive ligand-receptor interaction and calcium signaling pathway (Fig. 4C). Conversely, the down-regulated DEGs were mainly enriched in pathways such as cytokine-cytokine receptor interaction, JAK-STAT signaling pathway, RIG-I-like receptor signaling pathway, and other pathways (Fig. 4D).

**The PI3K-AKT signaling pathway is an important potential regulatory pathway for inhibiting PEDV CV777 strain infection through butyrate treatment**

In this study, the aim was to investigate the potential mechanism by which butyrate inhibits PEDV infection in IPEC-J2 cells. To achieve this, the DEGs were analyzed between the group pretreated with butyrate and infected with PEDV, and the group infected with PEDV without pretreatment. The thresholds of *P*-adjust value < 0.05 and  $|\log_2\text{fold change}| > 2$  were set. It was found that a total

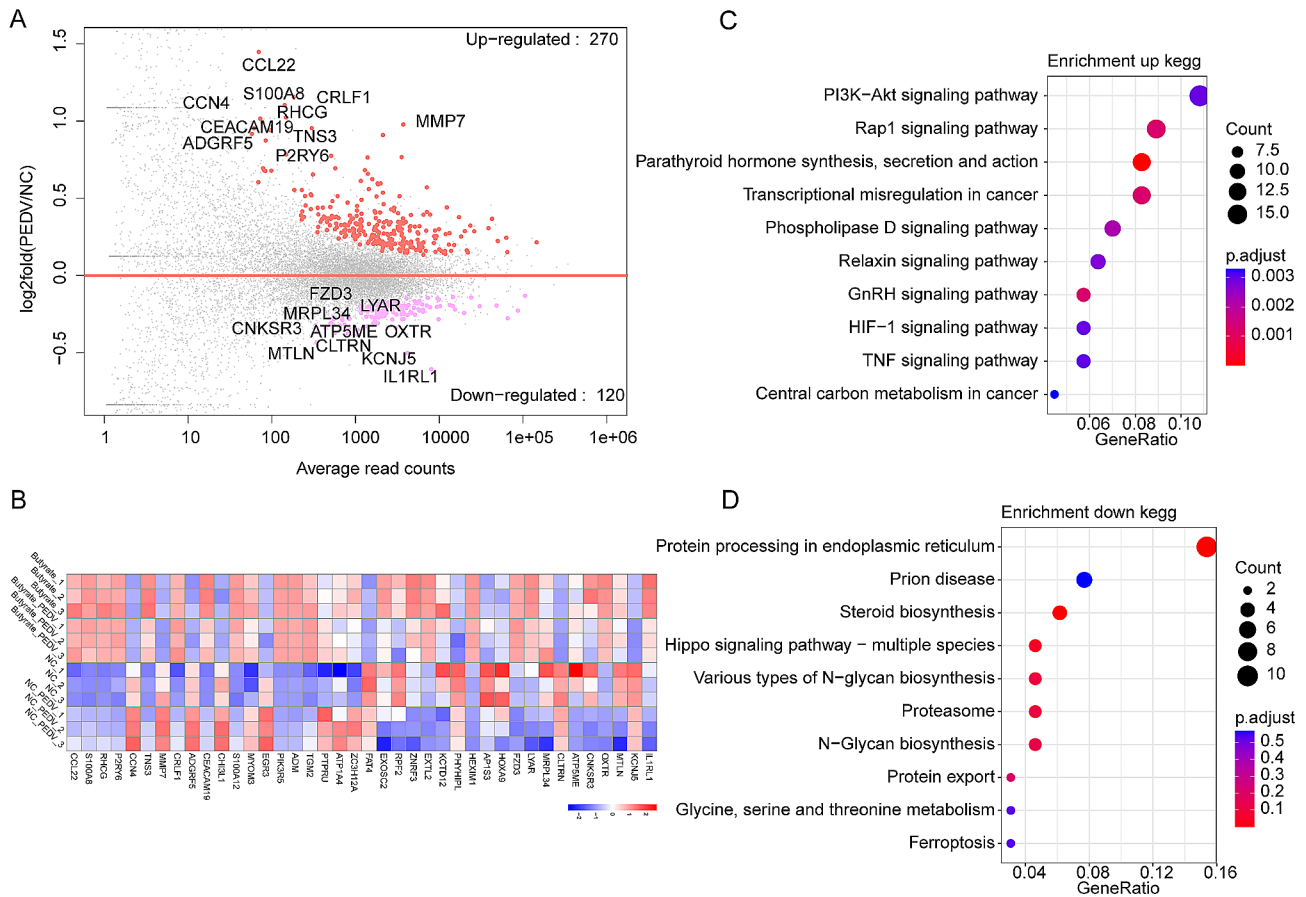


**Fig. 3** Illustrates the alterations in gene transcription observed in IPEC-J2 cells following infection with PEDV. **(A)** M-versus-A plot (MA) of DEGs between the PEDV-infected group and the NC group. Red dots represent up-regulated differentially expressed genes, pink dots represent down-regulated differentially expressed genes, and gray dots represent genes that are not significantly different. Horizontal coordinates represent average read counts, while vertical coordinates represent log<sub>2</sub>-transformed multiplicity of differences. **(B)** Heatmap of top 20 up-regulated and down-regulated DEGs, respectively. Bar represents the gene expression level after homogenization treatment. **(C)** KEGG enrichment analysis of up-regulated DEGs between the PEDV-infected group and the NC group. **(D)** KEGG enrichment analysis of down-regulated DEGs between the PEDV-infected group and the NC group

of 1,393 up-regulated DEGs and 255 down-regulated DEGs were detected (Fig. 5A). Cluster analysis revealed that these DEGs are also mainly influenced by the administration of butyrate (Fig. 5B). Subsequent enrichment analysis of these up-regulated DEGs demonstrated that they were predominantly enriched in pathways such as neuroactive ligand-receptor interaction, calcium signaling pathway, cAMP signaling pathway, and other pathways, etc. (Fig. 5C). Conversely, the down-regulated DEGs were mainly enriched in pathways such as Cytokine-cytokine receptor interaction, JAK-STAT signaling pathway, TGF-beta signaling pathway (Fig. 5D). These pathways may play a potential role in the inhibition of PEDV infection by butyrate. Further, by overlapping the up-regulated DEGs after butyrate treatment and the up-regulated DEGs after PEDV infection, a total of 33 genes were identified. The heatmap analysis revealed that these up-regulated DEGs exhibited a higher expression trend (Fig. 6A). On the other hand, the down-regulated DEGs after butyrate treatment and PEDV infection were also

overlapped, resulting in the identification of 4 genes that showed a lower expression trend after butyrate treatment (Fig. 6B). Furthermore, KEGG enrichment analysis of these overlapped genes indicated that they were primarily enriched in the PI3K-AKT signaling pathway (Fig. 6C), which was also up-regulated after PEDV infection (Fig. 3C). These findings suggest that butyrate may inhibit PEDV infection through modulation of the PI3K-AKT signaling pathway.

### Discussion

Butyrate, a carbon short-chain fatty acid synthesized by intestinal microorganisms through the metabolism of fiber, is present in the colon at concentrations reaching up to 140 mM [15], while in the jejunum, the concentration of butyric acid is around 5 mM [16]. It has been widely recognized for its potential to confer health benefits to humans, primarily through its anti-inflammatory properties. However, it has been suggested that butyrate may facilitate the replication of herpesviruses [17] as well



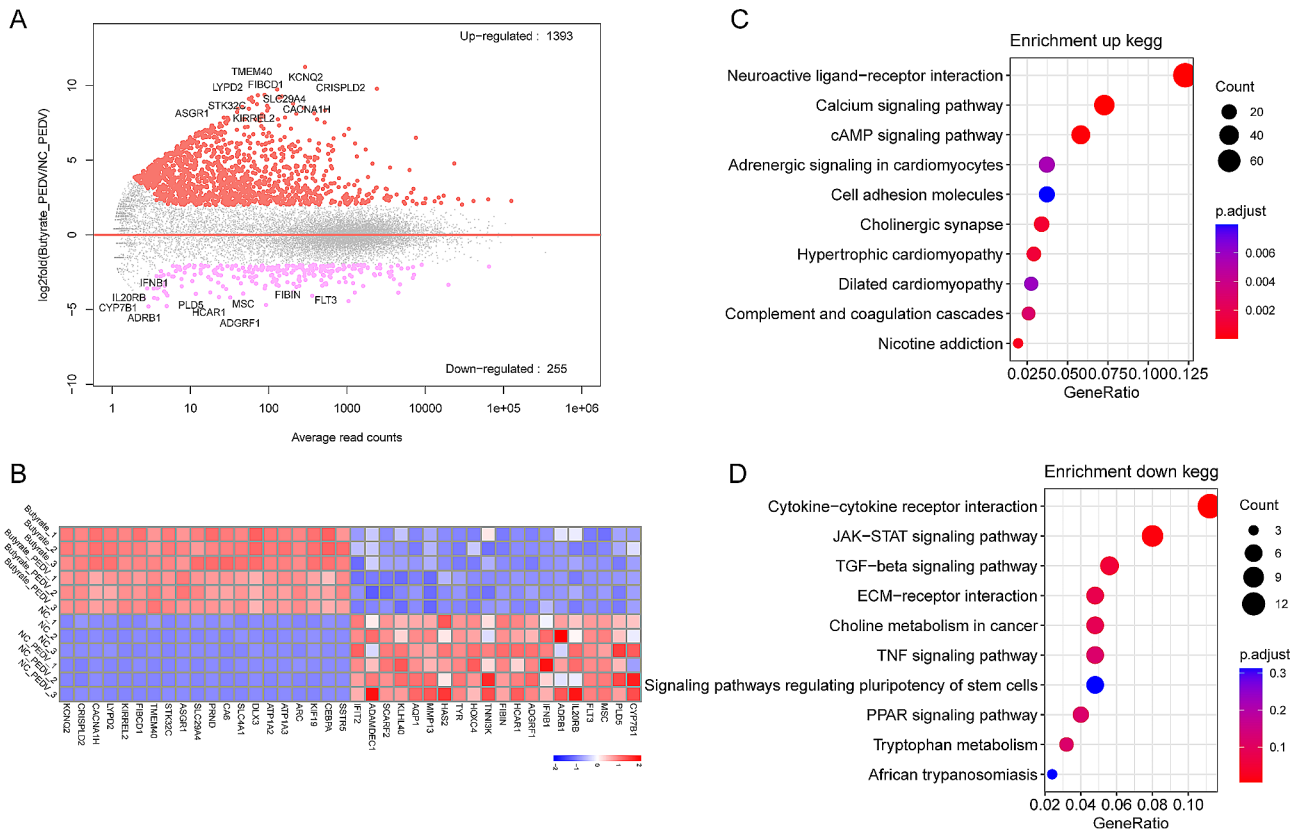


**Fig. 5** Effect of butyrate treatment on gene transcription to inhibit PEDV infection in IPEC-J2 cells. **(A)** M-versus-A plot (MA) of DEGs between the the group pretreated with butyrate and infected with PEDV, and the group infected with PEDV without pretreatment. **(B)** Heatmap of top 20 up-regulated and down-regulated DEGs, respectively. **(C)** KEGG enrichment analysis of up-regulated DEGs between the the group pretreated with butyrate and infected with PEDV, and the group infected with PEDV without pretreatment. **(D)** KEGG enrichment analysis of down-regulated DEGs between the group pretreated with butyrate and infected with PEDV, and the group infected with PEDV without pretreatment

were identified compared to those identified in response to PEDV infection. Furthermore, a majority of the genes exhibited an up-regulation trend following butyrate treatment. In contrast, PEDV infection did not exert as pronounced an effect on host genes as butyrate treatment, possibly due to the extensive host evasion mechanism employed by PEDV [30]. Our analysis of the DEGs indicated that several signaling pathways, including the JAK-STAT signaling pathway, ECM-receptor signaling pathway, RIG-I-like receptor signaling pathway, and TNF signaling pathway, were down-regulated following treatment with butyrate. This finding suggests that butyrate treatment may have an inhibitory effect on immune-related signaling pathways. It has been reported that the administration of butyrate resulted in an increase in the expression of over 800 genes. However, it was observed that butyrate strongly inhibited the expression of 60% of ISGs, while up-regulating 3% of ISGs [31]. These findings are consistent with the results obtained in the present study, suggesting that this may represent a novel mechanism through which butyrate exerts its effects on virus-infected cells.

To further investigate the potential targets of butyrate affecting PEDV infection, the DEGs were analyzed between the group pretreated with butyrate and infected with PEDV, and the group infected with PEDV without pretreatment. We found that these DEGs were enriched by pathways such as cytokine receptor interaction, JAK-STAT signaling pathway, neuroactive ligand-receptor interaction, and calcium signaling pathway. We found that the pathways enriched were similar to those enriched in the differential genes between the butyrate-treated and control groups. We hypothesized that this similarity might be attributed to the broader transcriptional changes induced by butyrate treatment. It is still debatable whether these pathways are associated with the inhibition of PEDV infection. Therefore, to further explore the differentially expressed genes and signaling pathways associated with the inhibition of PEDV infection by butyric acid, we analyzed the intersection of DEGs across various groups. The analysis revealed 37 genes that were found to be overlapped, and these genes were primarily enriched in the PI3K-AKT signaling pathway. It is worth noting that the PI3K/Akt signaling pathway has been

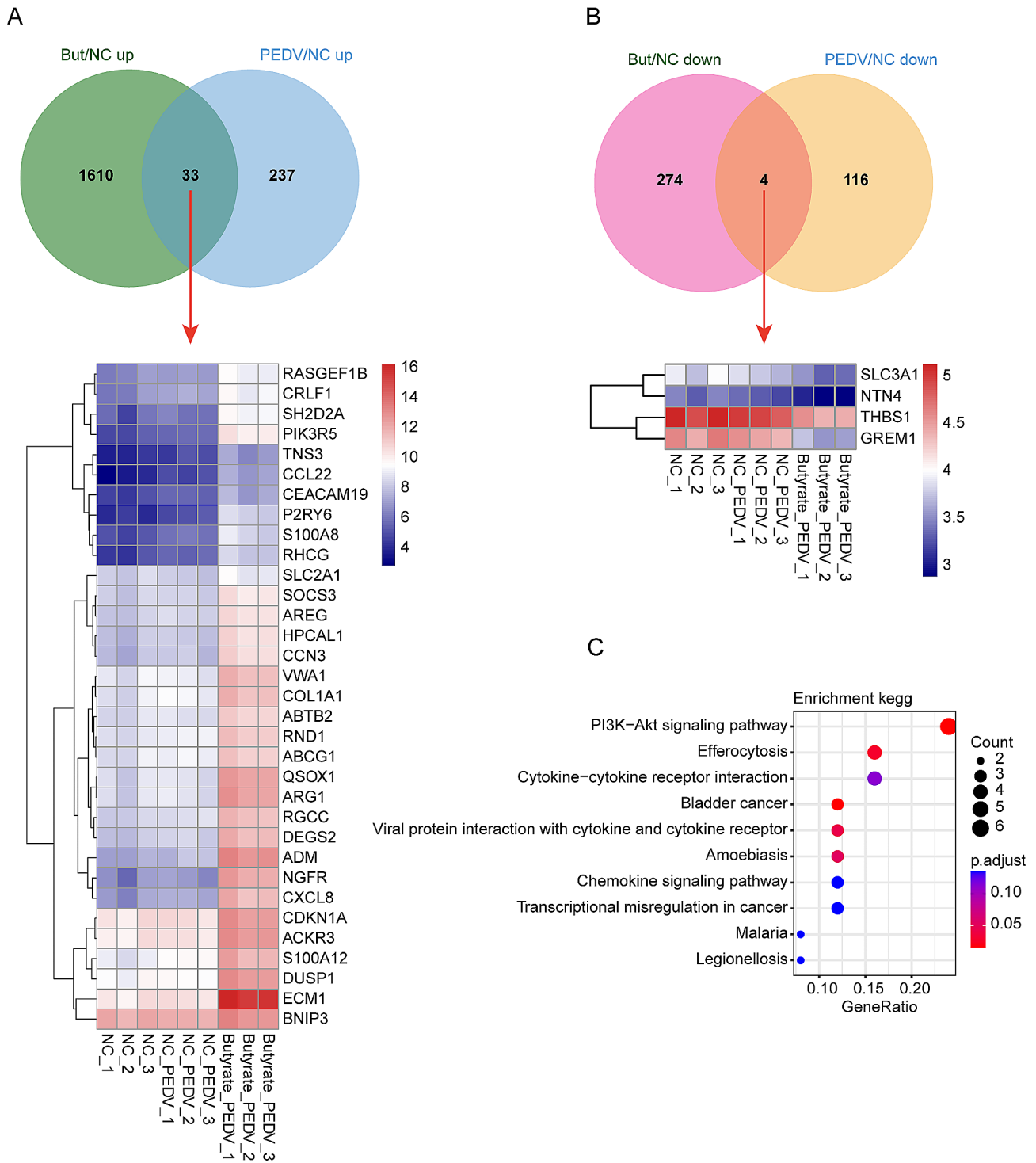


**Fig. 6** Overlap analysis for screening candidate regulatory genes. **(A)** Overlapped up-regulated genes in both the butyrate-treated and the PEDV-infected groups compared with the NC group. **(B)** Overlapped down-regulated genes in both the butyrate-treated and the PEDV-infected groups compared with the NC group. Heatmap below the Venn diagram represents the overlapped genes expression in different groups. **(C)** KEGG enrichment analysis of overlapped genes

reported to be up-regulated after PEDV infection and can inhibit PEDV replication [32]. However, it has also been reported that the PEDV nps6 protein of porcine epidemic diarrhea virus induces autophagy to promote viral replication through the PI3K/Akt/mTOR axis [33]. While there may be some discrepancies between the findings of these two studies, the military study demonstrated the significant involvement of the PI3K-AKT signaling pathway in PEDV infection. Butyrate might enhance tight junction protein abundance through mechanisms that include activation of AKT/mTOR-mediated protein synthesis [34]. This may be one of the reasons why high concentrations of butyrate can resist PEDV infection. This suggests that the PI3K-AKT signaling pathway may be one of the key pathways involved in the inhibition of PEDV replication by butyrate. Of course, there may be additional pathways and genes that are potentially significant targets for butyrate in regulating PEDV infection. However, further experimental evidence is required to substantiate these claims.

## Conclusion

This study presents evidence that Short-chain fatty acids inhibit PEDV CV777 strain replication, with butyrate being one of the most effective. butyrate has the potential to confer protection against PEDV CV777 strain infection in intestinal epithelial cells. Additionally, it sheds light on the host transcriptional profile of PEDV CV777 strain infection, which is found to be suppressed by butyrate. Our research indicates that the PI3K-AKT signaling pathway may play a potential role in mediating the regulatory effects of butyrate. This pathway could potentially serve as a novel strategy to inhibit PEDV infection through the actions of butyrate.

## Abbreviations

PEDV	Porcine epidemic diarrhea virus
PED	Porcine epidemic diarrhea
SCFAs	Short-chain fatty acids
IPEC-J2	Porcine small intestinal epithelial cells
MOI	Multiplicity of infection
Hpi	Hours post-infection
cDNA	Complementary DNA
RT-qPCR	Real-time quantitative PCR
PCA	Principal component analysis
DEGs	Differentially expressed genes
KEGG	Kyoto Encyclopedia of Genes and Genomes
IFN	Interferon
ISGs	Interferon-stimulated genes

## Acknowledgements

Not applicable.

## Author contributions

J.Y.W. conceived and designed the experiments. Z.Z. and Y.Q.Z. performed the experiments. X.T.Z. and C.B.Z. analyzed the data. Z.Z. and S.B.Z. wrote the paper. All authors read and approved the final version of the paper.

## Funding

This work was supported by the Natural Science Foundation of Jiangsu Higher Education Institutions (23KJB230004), the Phoenix Talent Project of Taizhou (2023) and the Natural Science Foundation of Jiangsu Agri-animal Husbandry Vocational College (NSF2023CB01).

## Data availability

No datasets were generated or analysed during the current study.

## Declarations

### Ethics approval and consent to participate

All the experiments that involved animals were carried out in accordance with the approved guidelines by the Ministry of Agri-culture and Rural Affairs of the People's Republic of China. The Ethics Committee of Jiangsu Agri-animal Husbandry Vocational College specifically approved this study.

### Consent for publication

Not applicable.

### Competing interests

The authors declare no competing interests.

Received: 25 February 2024 / Accepted: 3 July 2024

Published online: 11 July 2024

## References

- Li J, Murtaugh MP. Dissociation of porcine reproductive and respiratory syndrome virus neutralization from antibodies specific to major envelope protein surface epitopes. *Virology*. 2012;433:367–76.
- Stevenson GW, Hoang H, Schwartz KJ, Burrough ER, Sun D, Madson D, Cooper VL, Pillatzki A, Gauger P, Schmitt BJ, et al. Emergence of porcine epidemic diarrhea virus in the United States: clinical signs, lesions, and viral genomic sequences. *J Vet Diagn Invest*. 2013;25:649–54.
- Deng F, Ye G, Liu Q, Navid MT, Zhong X, Li Y, Wan C, Xiao S, He Q, Fu ZF, et al. Identification and comparison of receptor binding characteristics of the spike protein of two porcine epidemic Diarrhea Virus strains. *Viruses*. 2016;8:55.
- Song D, Moon H, Kang B. Porcine epidemic diarrhea: a review of current epidemiology and available vaccines. *Clin Exp Vaccine Res*. 2015;4:166–76.
- Zuo T, Liu Q, Zhang F, Lui GCY, Tso EYK, Yeoh YK, Chen ZG, Boon SS, Chan FKL, Chan PKS, et al. Depicting SARS-CoV-2 faecal viral activity in association with gut microbiota composition in patients with COVID-19. *Gut*. 2021;70:276–84.
- Dumas A, Bernard L, Poquet Y, Lugo-Villarino G, Neyrolles O. The role of the lung microbiota and the gut-lung axis in respiratory infectious diseases. *Cell Microbiol*. 2018;20:e12966.
- Gu S, Chen Y, Wu Z, Chen Y, Gao H, Lv L, Guo F, Zhang X, Luo R, Huang C, et al. Alterations of the gut microbiota in patients with Coronavirus Disease 2019 or H1N1 influenza. *Clin Infect Dis*. 2020;71:2669–78.
- Morrison DJ, Preston T. Formation of short chain fatty acids by the gut microbiota and their impact on human metabolism. *Gut Microbes*. 2016;7:189–200.
- Corrêa RO, Fachi JL, Vieira A, Sato FT, Vinolo MAR. Regulation of immune cell function by short-chain fatty acids. *Clin Transl Immunol*. 2016;5:e73.
- Myhrstad MCW, Tunsjo H, Charnock C, Telle-Hansen VH. (2020) Dietary Fiber, gut microbiota, and metabolic regulation-current status in human randomized trials. *Nutrients* 12.
- Silva YP, Bernardi A, Frozza RL. The role of short-chain fatty acids from gut microbiota in Gut-Brain communication. *Front Endocrinol*. 2020;11:25.
- He HY, Fan XL, Shen HY, Gou HC, Zhang CH, Liu ZC, Zhang B, Wuri N, Zhang JF, Liao M et al. (2023) Butyrate limits the replication of porcine epidemic diarrhea virus in intestine epithelial cells by enhancing GPR43-mediated IFN-III production. *Front Microbiol* 14.
- Qin W, Qi X, Xie Y, Wang H, Wu S, Sun MA, Bao W. LncRNA446 regulates tight junctions by inhibiting the Ubiquitinated Degradation of Alix after Porcine Epidemic Diarrhea Virus infection. *J Virol*. 2023;97:e0188422.
- Yang YH, Dudoit S, Liu P, Lin DM, Peng V, Ngai J, Speed TP. Normalization for cDNA microarray data: a robust composite method address missing single and multiple slide systematic variation. *Nucleic Acids Res* 30:e15.

15. Cummings JH, Pomare EW, Branch WJ, Naylor CP, Macfarlane GT. Short chain fatty acids in human large intestine, portal, hepatic and venous blood. *Gut*. 1987;28:1221–7.
16. Biagi G, Piva A, Moschini M, Vezzali E, Roth FX. Effect of gluconic acid on piglet growth performance, intestinal microflora, and intestinal wall morphology. *J Anim Sci*. 2006;84:370–8.
17. Saemundsen AK, Kallin B, Klein G. Effect of n-butyrate on cellular and viral DNA synthesis in cells latently infected with Epstein-Barr virus. *Virology*. 1980;107:557–61.
18. Miller CA, Carrigan DR. Reversible repression and activation of measles virus infection in neural cells. *Proc Natl Acad Sci U S A*. 1982;79:1629–33.
19. Pauli G, Ludwig H. Increase of virus yields and releases of Borna Disease virus from persistently infected cells. *Virus Res*. 1985;2:29–33.
20. Olsen JC, Sechelski J. Use of sodium butyrate to enhance production of retroviral vectors expressing CFTR cDNA. *Hum Gene Ther*. 1995;6:195–202.
21. Trompette A, Gollwitzer ES, Pattaroni C, Lopez-Mejia IC, Riva E, Pernot J, Ubags N, Fajas L, Nicod LP, Marsland BJ. Dietary Fiber confers Protection against Flu by shaping Ly6c<sup>+</sup> patrolling Monocyte Hematopoiesis and CD8<sup>+</sup> cell metabolism. *Immunity*. 2018;48:992–e10051008.
22. Feng WQ, Wu YC, Chen GX, Fu SP, Li B, Huang BX, Wang DL, Wang W, Liu JX. Sodium Butyrate attenuates Diarrhea in Weaned piglets and promotes tight Junction protein expression in Colon in a GPR109A-Dependent manner. *Cell Physiol Biochem*. 2018;47:1617–29.
23. Antunes KH, Fachi JL, de Paula R, da Silva EF, Pral LP, dos Santos AA, Dias GBM, Vargas JE, Puga R, Mayer FQ et al. (2019) Microbiota-derived acetate protects against respiratory syncytial virus infection through a GPR43-type 1 interferon response. *Nat Commun* 10.
24. Wang HF, Yang L, Qu H, Feng HY, Wu SL, Bao WB. (2019) Global mapping of H3K4 trimethylation (H3K4me3) and transcriptome analysis reveal genes involved in the response to Epidemic Diarrhea Virus infections in pigs. *Animals-Basel* 9.
25. Shi XJ, Zhang Q, Wang JJ, Zhang YT, Yan YC, Liu Y, Yang NL, Wang QQ, Xu XG. (2022) Differential expression analysis of mRNAs, lncRNAs, and miRNAs expression profiles and construction of ceRNA networks in PEDV infection. *Bmc Genomics* 23.
26. Zhang Y, Chen HJ, Yu J, Feng R, Chen Z, Zhang XL, Ren YD, Yang GJ, Huang XD, Li GX. (2022) Comparative transcriptomic analysis of porcine epidemic diarrhea virus epidemic and classical strains in IPEC-J2 cells. *Vet Microbiol* 273.
27. Hu ZZ, Li YC, Du H, Ren JX, Zheng XR, Wei KJ, Liu JF. (2020) Transcriptome analysis reveals modulation of the STAT family in PEDV-infected IPEC-J2 cells. *Bmc Genomics* 21.
28. Shen XH, Yin L, Pan XC, Zhao RJ, Zhang DJ. (2020) Porcine epidemic diarrhea virus infection blocks cell cycle and induces apoptosis in pig intestinal epithelial cells. *Microb Pathogenesis* 147.
29. Zhang HW, Liu QF, Su WW, Wang JK, Sun YR, Zhang JF, Shang K, Chen ZH, Cheng SP, Wu H. Genome-wide analysis of differentially expressed genes and the modulation of PEDV infection in Vero E6 cells. *Microb Pathogenesis*. 2018;117:247–54.
30. Koonpaew S, Teeravechyan S, Frantz PN, Chailangkarn T, Jongkaewwattana A. PEDV and PDCoV Pathogenesis: the interplay between host Innate Immune responses and porcine enteric coronaviruses. *Front Vet Sci*. 2019;6:34.
31. Chemudupati M, Kenney AD, Smith AC, Fillinger RJ, Zhang LZ, Zani A, Liu SL, Anderson MZ, Sharma A, Yount JS. (2020) Butyrate reprograms expression of specific Interferon-stimulated genes. *J Virol* 94.
32. Kong N, Wu YG, Meng Q, Wang ZZ, Zuo YW, Pan X, Tong W, Zheng H, Li GX, Yang S et al. (2016) Suppression of virulent porcine epidemic Diarrhea Virus Proliferation by the PI3K/Akt/GSK-3 $\alpha$ / $\beta$  pathway. *Plos One* 11.
33. Lin HX, Li B, Liu MX, Zhou H, He KW, Fan HJ. (2020) Nonstructural protein 6 of porcine epidemic diarrhea virus induces autophagy to promote viral replication via the PI3K/Akt/mTOR axis. *Vet Microbiol* 244.
34. Yan H. Ajuwon KM Butyrate modifies intestinal barrier function in IPEC-J2 cells through a selective upregulation of tight junction proteins and activation of the akt signaling pathway. *PLoS ONE* 12:e0179586.

#### Publisher's Note

Springer Nature remains neutral with regard to jurisdictional claims in published maps and institutional affiliations.